Available online at www.sciencedirect.com
ScienceDirect
Journal of the European Ceramic Society 30 (2010) 61–72
www.elsevier.com/locate/jeurceramsoc

Effect of dopants on the phase stability of zirconia-based plasma sprayed thermal barrier coatings

S.A. Tsipas *

Dpto. Ciencia e Ingeniería de Materiales e Ingeniería Química, IAAB, Universidad Carlos III de Madrid, Avda. de la Universidad, 30, 28911 Leganés, Madrid, Spain

Received 3 September 2008; received in revised form 23 July 2009; accepted 7 August 2009
Available online 2 September 2009

Abstract

The influence of stabilizer type on the phase stability of thermal barrier coatings (TBCs) produced by air plasma spraying was explored. Together with the widely used zirconia-stabilized with yttria, other novel compositions, such as dysprosia-stabilized zirconia, yttria–lanthana-stabilized zirconia and ceria-stabilized zirconia were also investigated. The effect of isothermal heat treatment on the phase stability was explored. Results suggest that decomposition of the "non-transformable" tetragonal phase occurs to a greater or lesser extent for all dopants at these temperatures. The effect of Al_2O_3 and SiO_2 content was also explored. The rate of decomposition depends on the dopant kind, amount and on the presence of Al_2O_3 and SiO_2 impurities.

Keywords: Thermal barrier coatings; X-ray methods; ZrO_2; Impurities; Al_2O_3

1. Introduction

The application of TBCs on metallic structures of the hot section of land-based/aero gas turbines offers many benefits in terms of increases in operating temperatures, increased efficiency, enhanced component durability and reduced cooling requirements to metallic components. TBCs comprise of a two layer structure: (i) a bond coat (BC), an oxidation-resistant metallic layer which is applied to the superalloy or other material substrate that carries the structural load and (ii) a top coat (TC), a porous ceramic layer that acts as the insulator and between the substrate and the environment. The conventional material used for the TC in TBCs is ZrO_2 stabilized with 7–9 wt% Y_2O_3. Phase stability of the TC is of great importance for the durability and reliability of TBCs. Zirconia exists as three solid phases that are stable at different temperatures.[1] At temperatures up to 1200 °C, the monoclinic phase (*m*) is stable. Zirconia transforms from the monoclinic to the tetragonal phase (*t*) above 1200 °C and above 2370 °C to the cubic phase (*c*). Transformation from *m* to the *t*-phase has an associated volume decrease of 4%. Zirconia-based TBCs are doped with trivalent or tetravalent cations, in order to stabilize the tetragonal zirconia polymorph and prevent catastrophic cracking as a result of the volume changes accompanying the $t \rightarrow m$ transformation, which occurs at temperatures within the range of the working environment in gas turbines. The polymorphism of zirconia has led to the investigation of various stabilized zirconia alloys.[2] The phase constitution of zirconia-based TBCs is controlled by many factors such as stabilizer content, processing parameters and heat treatment. The phase stability of the top coat constitutes an important factor for determining the thermomechanical properties of TBCs.

TBCs are commonly applied by plasma spraying. Plasma sprayed (PS) top coats of partially stabilized zirconia with 8 wt% yttria consist of non-transformable metastable t' tetragonal phase. A metastable tetragonal phase (t') results from a diffusionless shear transformation directly from the cubic state. During plasma spraying, the rapid cooling of molten splats to the substrate temperature often results in the formation of t' phase. This phase is thought to be stable up to 1400 °C, i.e. it does not transform directly to monoclinic on cooling to room temperature.

Stabilization of the tetragonal or cubic zirconia phase by the addition of trivalent dopants is believed to be associated

* Tel.: +34 91 6248374; fax: +34 91 6249430.
E-mail address: stsipas@ing.uc3m.es.

0955-2219/$ – see front matter © 2009 Elsevier Ltd. All rights reserved.
doi:10.1016/j.jeurceramsoc.2009.08.008

with the generation of oxygen vacancies.[3] The trivalent dopant cations substitute the Zr ion in the cation network and oxygen vacancies are created for charge compensation. The tetragonal and cubic polymorphs are stabilized when the doping level is sufficient to create enough oxygen vacancies to reduce the co-ordination number of the Zr ion from 8 to around 7.5.[4,5] The Zr ion in fully stabilized and high temperature cubic phase has a co-ordination number of 7, due to the strong covalent nature of the Zr–O bond and the small size of the Zr ion.

The phase stability of PS top coats after prolonged heat treatment is an important issue. Different stabilizers have been used to ensure that the tetragonal phase is retained. Early attempts used MgO to stabilize zirconia in its cubic state, by adding 25 wt% MgO.[6] However, during heat treatment the zirconia reverts to its monoclinic form and the stabilizing oxide precipitates out from solid solution, affecting the thermal conductivity.[7] Zirconia can be fully stabilized to its cubic phase by adding 20 wt% yttria. However, such fully stabilized zirconia coatings perform very poorly in thermal cycling tests.[8]

CeO_2-stabilized TBCs have been investigated by various researchers[9–13] and the existence of the non-transformable t' tetragonal phase similar to that in the YSZ has been agreed upon. At high CeO_2 weight percentages a second metastable cubic phase c' also exists. In reducing atmospheres the Ce^{4+} ion reduces to Ce^{3+}, which tends to stabilize the cubic phase.[14]

Gadolinia is in general a less effective stabilizer than yttria, although partial substitution of Gd for Y does enhance phase stability, if Y remains the dominant species.[15,16] ZrO_2–Er_2O_3, ZrO_2–Sm_2O_3 and ZrO_2–Nd_2O_3 PS TBCs have been reported to consist of non-transformable t' tetragonal phase up to compositions of 6 mol.% of stabilizer, and above that, coatings are entirely cubic.[17–19] Erbia-stabilized coatings showed better thermal phase stability than samaria-stabilized and neodymia-stabilized coatings, which decomposed after heat treatment to the monoclinic and tetragonal phases. Scandia–yttria-stabilized TBCs have been reported to show better phase stability than conventional YSZ TBCs up to temperatures of 1400 °C.[20,21] Dy_2O_3 and Yb_2O_3 rare-earth dopants have also been reported to stabilize the tetragonal phase.[22,23] Zirconia doped with lanthana has been reported to form the cubic pyrochlore-structured phase, especially at high mol % of stabilizer.[24–26] The cubic pyrochlore-structure is stable up to its melting point and hence it is believed that these materials might have potential as TBCs.[27] However coatings of this material yield shorter thermal fatigue cyclic life than YSZ due to their relatively low CTE.[28]

The scope of this work is to determine the phase constitution of zirconia-based plasma sprayed top coats doped with yttria, dysprosia, yttria–lanthana and ceria, assess the ability of the different dopants to stabilize the tetragonal phase t' and quantify the rate of decomposition after heat treatment. In this paper not only the effect of stabilizer and heat treatment is explored but also in addition, the effect of common impurities present in YSZ, such as Al_2O_3 and SiO_2 is described. The results are discussed with relevance to the use of these coatings in TBC applications.

Table 1
Compositions for the top coat powders.

Product	Composition	Acronym
204NS-1	Yttria-stabilized zirconia	YSZ
204NS	Yttria-stabilized zirconia	YSZ
205NS	Ceria-stabilized zirconia	CSZ
SPM6-2444	Dysprosia-stabilized zirconia	DSZ
AE8321	Yttria–lanthana-stabilized zirconia	YLSZ
AE8170	Al_2O_3-doped yttria-stabilized zirconia	Al_2O_3-doped-YSZ
AE9018	Al_2O_3-doped yttria-stabilized zirconia	Al_2O_3-doped-YSZ

2. Experimental procedure

Specimens were produced by air plasma spraying (APS) onto mild steel substrates of 1.5 mm thickness. Details of the spraying conditions can be found elsewhere.[29] The powders utilised were supplied by Sultzer Metco Inc. (Westbury, NY). A summary of compositions and acronyms of the top coat powders is presented in Table 1. Chemical compositions of powders, as given by the supplier, are summarized in Table 2.

X-ray diffraction (XRD) measurements were carried out using a computer-controlled Phillips PW1710 diffractometer, with Cu Kα radiation (λ = 0.154 nm), 40 kV accelerating current and a 40 mA filament current. The incident beam optical conditions were set up with an anti-scatter slit of 1° and a 15 mm horizontal mask. For the diffracted beam, a 0.2 mm receiving slit and a 1° divergence slit were used. The apparatus was regularly calibrated using a silicon control sample.

Scans over the range $2\theta = 25$–$80°$ were carried out with a step size of 0.02° and 4 s counting time at each step. Two regions were of particular interest for the identification of the phases present. The first of these was the region $2\theta = 27$–$32°$, where $(\bar{1}\,1\,1)_m$ and $(1\,1\,1)_m$ peaks, and the $(1\,1\,1)_{cub/tet}$ peak are found. Slow scans were performed over this range, with a step size of 0.02° and a dwell time of 10 s. The second region examined by a slow scan was $2\theta = 72$–$75°$, in order to examine the $(4\,0\,0)_{tet}$, $(0\,0\,4)_{tet}$ and the $(4\,0\,0)_{cub}$ peaks. Slow scans were performed over this range with a step size of 0.01° and a dwell time of 35 s.

The mole fractions of tetragonal, monoclinic and cubic phases were calculated from the peak intensities of the slow scans, using the following equation, from Miller et al.[30] and Toraya et al.[31,32]:

$$\frac{M_m}{M_c + M_t} = 0.82\left(\frac{I_{(\bar{1}\,1\,1)_m} + I_{(1\,1\,1)_m}}{I_{(1\,1\,1)_{c/t}}}\right) \quad (1)$$

$$\frac{M_c}{M_t} = 0.88\left(\frac{I_{(400)_c}}{I_{(004)_t} + I_{(400)_t}}\right) \quad (2)$$

$$M_m + M_c + M_t = 1 \quad (3)$$

where M_m, M_c and M_t are the mole fractions of the monoclinic, cubic and tetragonal phases, respectively, and I is the integrated intensity corresponding to the peak concerned. The integrated intensity was calculated after peak deconvolution and profile fitting, performed using Phillips PROFIT software. The software can fit Lorenzian, Gaussian, pseudo-Voigt and Pearson-Seven profiles, all of which can be symmetrical or asymmetric, and it

Table 2
Chemical composition of ceramic powders supplied by Sulzer Metco Inc.

Chemical composition (wt%)	Powder product						
	204NS-1	204NS	205NS	SPM6–2444	AE8312	AE8170	AE9018
Al_2O_3	0.01	<0.01	<0.01	0.02		0.88	0.8
CaO	0.04	<0.01		0.02	0.01	<0.01	<0.02
CeO_2			25.15			<0.02	<0.02
HfO_2	1.7	1.51	1.2	1.5	1.54	1.59	1.59
Dy_2O_3				10.1			
La_2O_3					6.58		
SiO_2	0.3	0.07	0.0	0.10	0.04	0.05	0.05
TiO_2	0.04	0.09	0.01	0.10	0.10	0.10	0.10
Y_2O_3	7.8	7.6	2.4		6.50	7.51	6.5
ZrO_2	Balance	Balance	Balance	Balance	Balance	Balance	Balance

will assign the $K\alpha_2$s. This procedure allows accurate determination of peak positions, peak areas and widths. The deconvolution of the XRD spectra in the region $2\theta = 72–75^\circ$ to determine the presence of the cubic and tetragonal phases was performed taking into consideration the ratio of relative intensities of the $(4\,0\,0)_{tet}$ and $(0\,0\,4)_{tet}$ peaks as given by the JCPDS files. Even though no constraint was applied during the deconvolution, the reported relative intensities for the 0 0 4 and 4 0 0 peaks were taken into consideration and it was cross-checked that for the deconvoluted profiles presented, the relative intensities between the two peaks are within the range reported in literature. The profile fitting that yielded the best fit, with the lowest differential plot and lowest R_{min} value (the integral value that shows the difference between the experimental and calculated profiles) is presented.

Alternative, quantitative phase analysis was in some cases performed with the full X-ray diffraction pattern, using the Rietveld method based on the Phillips X'pert Plus software. The Rietveld code in the software is based on.[33] In order to perform the analysis, all phases must be identified and the quality data for the structure of the phases present must be available. The Rietveld method permits simultaneous refinement in each of the present phases of both structural (lattice parameters) and microstructural (phase percentage) parameters.

The $(4\,0\,0)_{tet}$, $(0\,0\,4)_{tet}$ and $(4\,0\,0)_{cub}$ peak positions were used for calculation of lattice parameters, a for the cubic phase and a and c for the tetragonal phase. The Y_2O_3 content of the tetragonal and cubic phases were calculated from these measured lattice parameters, respectively using the following equations,[34] where a and c are expressed in nanometers

$$\text{mole.\% } YO_{1.5} \text{ in tetragonal phase} = \frac{1.0223 - (c/a)}{0.001309} \quad (4)$$

$$\text{mole.\% } YO_{1.5} \text{ in cubic phase} = \frac{a - 0.5104}{0.0204} \quad (5)$$

Samples top coats were debonded from their substrates and isothermal heat treatments were performed on free-standing APS top coats at temperatures in the range 1200–1400 °C. Samples were removed from the furnace once the heat treatment was completed and were air cooled at a rate of about 30 °C/min.

3. Results and discussion

3.1. As-sprayed

3.1.1. Yttria-stabilized zirconia top coats

The x-ray diffraction patterns of the as-sprayed top coats are presented in Fig. 1. The YSZ as-sprayed top coats (204NS & 204NS-1) are composed of non-transformable t' tetragonal phase. The $K\alpha_1$ and $K\alpha_2$ components of the t' peaks can be distinguished. The t' non-transformable tetragonal is not an equilibrium phase and it differs from the regular tetragonal phase, notably for its smaller tetragonality, higher yttria content and stability against further transformation into the monoclinic phase.[34–38] However, for crystallographic purposes, the t' non-transformable tetragonal phase and t tetragonal phase are

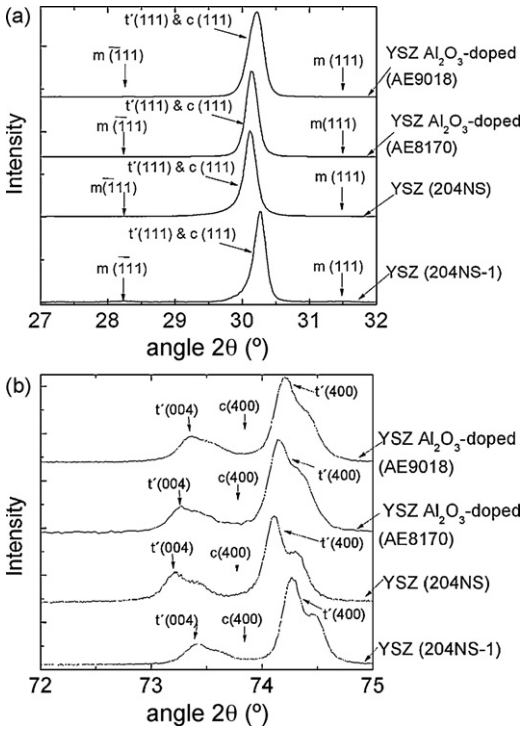

Fig. 1. XRD spectra in 2θ ranges of (a) 27–32°, and (b) 72–75° for as-sprayed YSZ (204NS-1), YSZ (204NS), Al_2O_3-doped-YSZ (AE8170) and Al_2O_3-doped-YSZ (AE9018) top coats.

fundamentally the same tetragonal polymorph in the zirconia solid solution.[39] The resistance of the non-transformable tetragonal to transformation into the monoclinic phase is ascribed to its smaller tetragonality. The position of the tetragonal peaks is known to move as a function of the amount of yttria that the tetragonal phase contains, due to the changing lattice parameter. Due to the slightly different yttria content, the tetragonal peaks are not in exactly the same position in the two coatings. Trace amounts of the monoclinic phase exist in the 204NS-1 YSZ powder (1.5%), which may be due to the presence of unmelted particles that could contain some monoclinic phase. The different amount of impurities in the starting powders 204NS and 204NS-1 of these two coatings does not have a noticeable effect of their phase constitution.

The two YSZ top coats doped with a small amount of Al_2O_3 (AE8170 & AE9018) also contain the non-transformable tetragonal phase. The shoulder observed on both the tetragonal peaks are due to the $K\alpha_1$ and $K\alpha_2$ components of the t' peaks. The presence of a small amount of Al_2O_3 does not appear to alter the phase constitution of the top coat. The solubility of Al_2O_3 in Zr_2O is very low[40,41] (<0.5 mol.%), so it is possible that the Al_2O_3 is not in solid solution. However the amount present is too small to form a distinct peak. It can be concluded that impurities such as SiO_2 and Al_2O_3 do not have an effect on the phase constitution of as-sprayed YSZ coatings.

3.1.2. Dysprosia-stabilized zirconia top coats

The DSZ top coat (SPM6-2444) in the present study, which has about 3.5 mol.% Dy_2O_3, comprises the non-transformable tetragonal t' with a trace of monoclinic phase (1.5%). No pyrochlore phase is observed. The $K\alpha_1$ and $K\alpha_2$ components of the t' peaks can be distinguished (Fig. 2). Dysprosia is also believed to be an effective stabilizer in zirconia, up to concentrations of about 15 mol.% (≈35 wt%).[42] When the concentration of Dy_2O_3 is above 15 mol.%, the pyrochlore-structure $Dy_2Zr_2O_7$ phase and zirconia solid solution are supposed to co-exist.

The tetragonality c/a is an important factor in the stability of the tetragonal phase and it has been shown to be independent of the species of the dopant, but dependant on the content of the dopant for oversized trivalent rare earths.[23,43] Tetragonality decreases with increasing dopant content for oversized trivalent cations and vanishes at 11 mol.% M_2O_3 regardless of the ionic sizes, since tetragonality is aided by the creation of oxygen vacancies only.[39] The mol.% dysprosia in the DSZ (3.58 mol.%) in the present study is slightly lower than that of yttria in the YSZ top coats (about 4.3 mol.%). Therefore, we expect the DSZ top coat will have a higher tetragonality than that of YSZ coatings ($c/a_{DSZ} = 1.012$, $c/a_{YSZ} = 1.010$). Differences in the stability of the tetragonal phases in zirconia have been ascribed to differences in tetragonality and the resistance of the non-transformable tetragonal to transformation into the monoclinic phase is attributed to its smaller tetragonality.[43] Hence decrease in tetragonality is associated with increasing stability of the tetragonal phase.

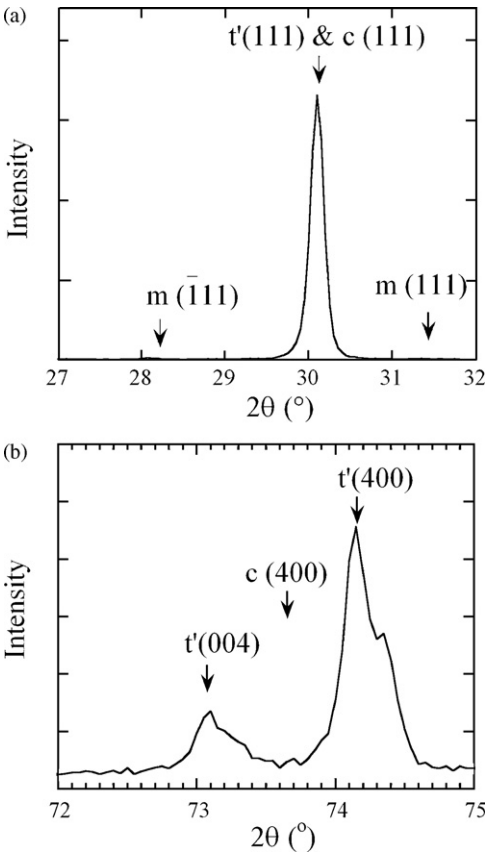

Fig. 2. XRD spectra in 2θ ranges of (a) 27–32°, and (b) 72–75° for as-sprayed DSZ (SPM6-2444) top coat.

3.1.3. Yttria–lanthana-stabilized zirconia top coats

For the YLaSZ, the deconvoluted spectrum is presented in Fig. 3b, which shows that the as-sprayed coating probably consists of two tetragonal phases with slightly different lattice parameters (deconvolution of the X-ray spectra considering a single tetragonal phase yielded a value of $R_{min} = 0.19\%$ whereas considering the presence of two tetragonal phases a much better fitting was achieved, $R_{min} = 0.04\%$). Possibly the presence of the two tetragonal phases is a result of two different dopants with different ionic radii. Whereas tetragonality is independent of ionic radius of the dopant and depends only on dopant content, on the other hand lattice parameters of the tetragonal phase increase systematically with the ionic radii of the dopant atoms.[23,43] If the two tetragonal phases that appear to be present are a result of the simultaneous presence of yttria and lanthana, then the tetragonal phase with the greater lattice parameters is a result of the lanthana dopant, whereas the tetragonal phase with slightly smaller lattice parameters is a result of the yttria dopant, since the lanthanum cation has a bigger ionic radius (see Table 3).

The stabilization effect of lanthana in zirconia is disputed in the literature. As the ionic size mismatch between the dopant

Table 3
Ionic radii for cations in PSZ top coats.[56].

Ion	Zr^{4+}	Y^{3+}	Dy^{3+}	La^{3+}	Ce^{4+}	Ce^{3+}
Ionic radius (nm)	0.084	0.102	0.103	0.116	0.097	0.114

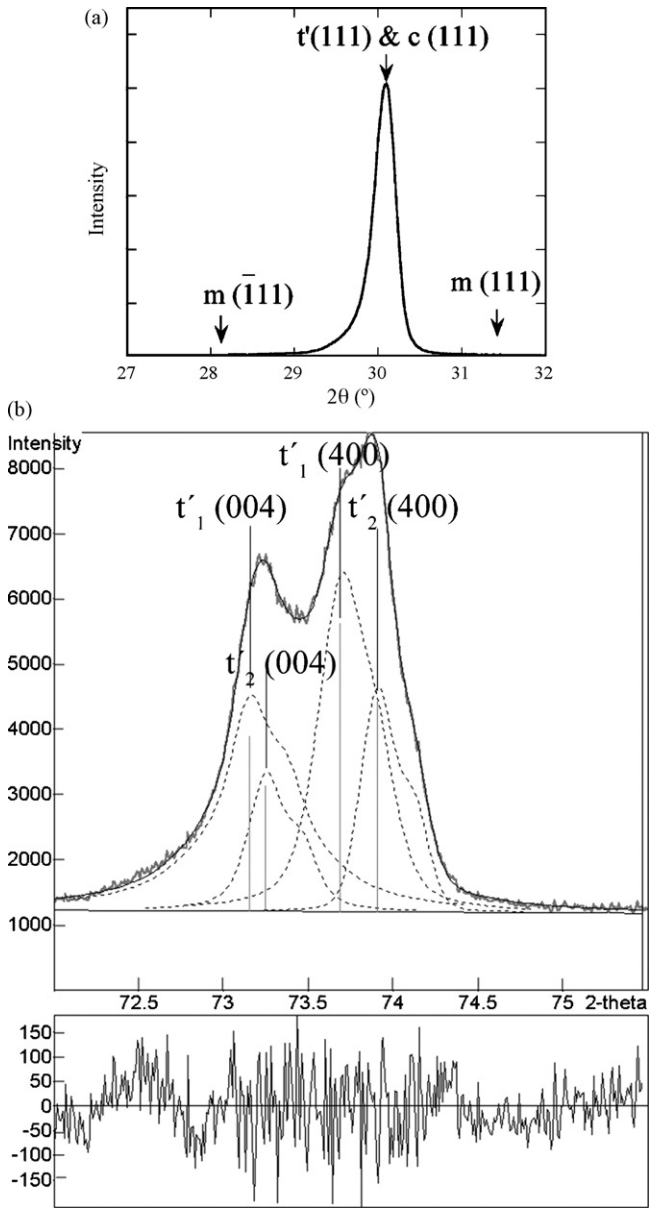

Fig. 3. XRD spectra in 2θ ranges of (a) 27–32°, and (b) 72–75° (deconvoluted) for as-sprayed YLSZ (AE8321) top coat. The differential (residual) plot for the deconvoluted profile is included (R_{min} = 0.04%).

and the zirconium atom becomes greater, the solubility of the tetragonal and cubic phase decreases and the pyrochlore phase may be formed instead of the tetragonal or cubic phase. According to the binary zirconia lanthana phase diagram[28] at above about 2 mol.% La the equilibrium phases are the monoclinic and the pyrochlore phase. No pyrochlore phase was detected in the present study in the as-sprayed coatings. Din and Kaleem[42] reported that the addition of lanthana to zirconia did not stabilize the *t*-phase. However, a pyrochlore-type cubic phase $La_2Zr_2O_7$ is formed. Bastide et al.[25] also found that the solid solubility of La in monoclinic Zr is 1.5 mol.% and above that concentration pyrochlore-structured $La_2Zr_2O_7$ phase is formed. However, Li et al.[44] reported that 8 mol.% La_2O_3 stabilized the tetragonal phase of La_2O_3–ZrO_2 powder compacts. In the present study the simultaneous presence of yttria and lanthana stabilizers in zirconia appears to result in two metastable tetragonal phases in the as-sprayed coatings.

3.1.4. Ceria-stabilized zirconia top coats

The CSZ powder also contains the non-transformable tetragonal phase (see Fig. 4). Tetravalent dopants such as ceria stabilize the tetragonal and cubic phases of zirconia.[9,45] However, the stabilization is not the result of the generation of oxygen vacancies, as is the case with trivalent dopants. The Ce^{4+} ion substitutes the Zr^{4+} ion in the cation network, without creating any oxygen vacancies, since both ions are tetravalent.[46,47] The stabilization effect is thought to be caused by the slight dilation of the cation network by the oversized Ce^{4+} ion which decreases the tetragonality and stabilizes the tetragonal phase to room temperature.[46] In Fig. 4 broad XRD peaks are observed for the CSZ top coat. This has commonly been observed previously with CSZ top coats. It is thought to relate to compositional variations, owing to the larger size of the Ce ion within the zirconia lattice.[11] Some research[14,48] suggests that the tetravalent Ce ion is reduced to is trivalent state because of the reducing atmosphere in the plasma plume and the rapid quenching thereafter of the molten droplets. In such situation, oxygen vacancies would be introduced to balance the lower valance state of the cerium ion. This would result in stabilization of the cubic phase and possibly the presence of both non-transformable tetragonal t' and cubic *c* phases. The presence of some trivalent cerium could account for the large variation in the unit cell and thus the broad XRD peaks observed. The presence of some cubic phase is also a possibility. However, the presence of a cubic peak cannot be confirmed in the data pre-

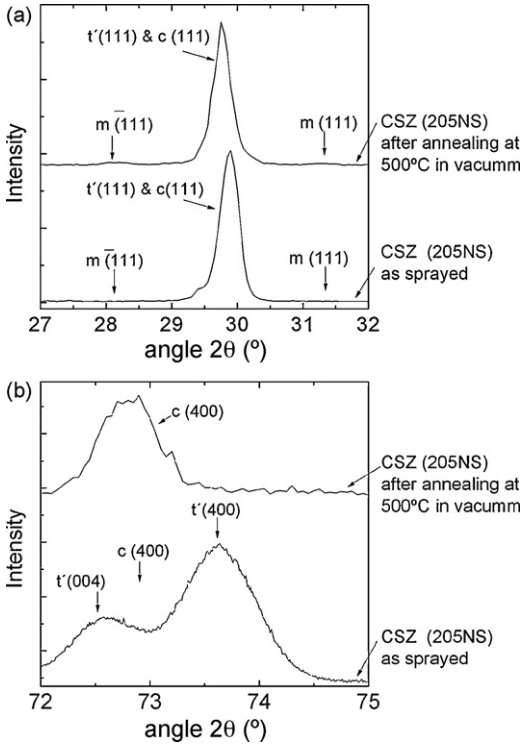

Fig. 4. XRD spectra in 2θ ranges of (a) 27–32°, and (b) 72–75° for as-sprayed CSZ (205NS) top coat and CSZ (205NS) top coat that has been annealed in vacuum at 500 °C.

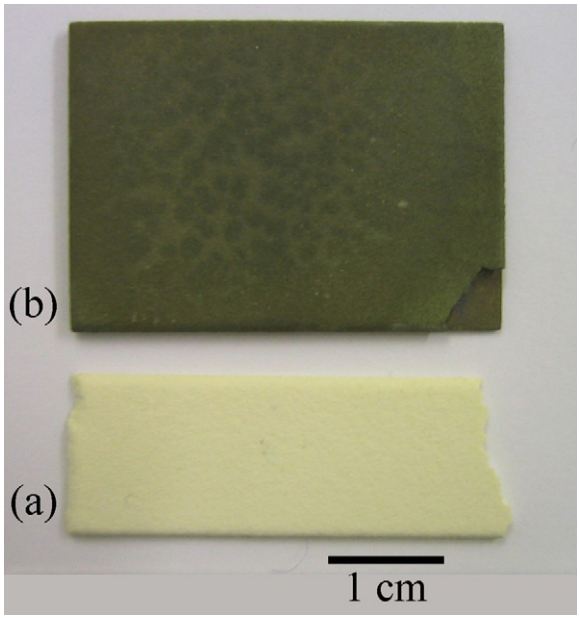

Fig. 5. CSZ (205NS) top coat (a) as-sprayed and (b) after annealing at 500 °C in vacuum. The change in color is due to reduction of Ce^{4+} to Ce^{3+}. (For interpretation of the references to color in this figure legend, the reader is referred to the web version of the article.)

sented here (see Fig. 4), since the height of any cubic peak is expected to be of the same order as the noise, even though the signal to noise ratio is satisfactory. Annealing at relatively moderate temperature (700 °C) should result in re-oxidation of the cerium into its tetravalent state and stabilization of the tetragonal phase, with no cubic phase present. The color of CSZ plasma sprayed coatings in which the cerium ion has been reduced to its trivalent state is brown–green,[9,10] whereas for CSZ coatings with the majority of the substitutional Ce ions in their tetravalent state the color is pale yellow.[9] The samples used in the present work were pale yellow in the as-sprayed state, further suggesting that they consist mainly of tetravalent cerium and non-transformable tetragonal phase t' (see Fig. 5). It is possible that trivalent cerium formed during spraying was re-oxidized during cool-down, since the plasma sprayed coatings were air cooled to below 120 °C inside the spraying chamber. Previous work[47] suggests that the ceria ions in CSZ plasma sprayed coatings are preferentially in their tetravalent state.

The reduction of cerium atoms to their trivalent state is accompanied by a volume change. The Ce^{3+} ion is larger than the Ce^{4+} ion, resulting in a decrease in the solubility of CeO_2 in the tetragonal solid solution and causing a decomposition in the *t*-phase. Fig. 4 shows X-ray spectra for CSZ after annealing at 500 °C in vacuum. The tetragonal phase has decomposed into cubic. In addition, the color of the as-sprayed coating changed to dark-brown/green (see Fig. 5), which suggests that the cerium cation has been reduced to its trivalent state. Dalmaschio et al.[14] noticed a volume diminution at 340 °C during cool-down, believed to be due to the phase transformation from cubic to tetragonal due to re-oxidation. The valance state of cerium in CSZ top coats is believed to have a large influence on the stress state in the ceramic coating.[14] The simultaneous presence of ceria and yttria makes it difficult to estimate the stabilizer content from the peak position, using known relations between lattice parameters and stabilizer percentage.

3.2. Isothermal heat treatment

3.2.1. Yttria-stabilized zirconia top coats

After holding the YSZ 204NS-1 top coat at 1300 °C for 100 h, the tetragonal t' phase decomposed to a mixture of low-yttria tetragonal t'_1, high-yttria cubic c and t'_2 with an intermediate yttria composition as shown in Fig. 6 (profile fitting of the X-ray spectra considering the cubic phase and a single tetragonal phase yielded a value of $R_{min} = 0.26\%$ whereas considering the presence of two tetragonal phases a much better fitting was achieved, $R = 0.02\%$). According to the phase diagram[49] YSZ top coats

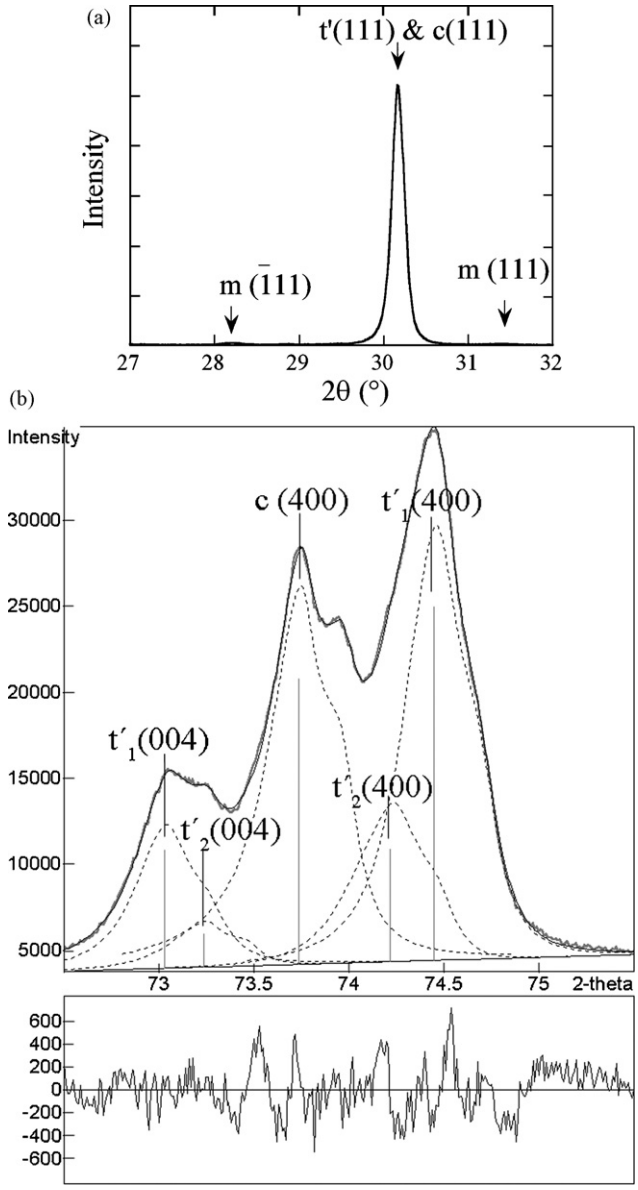

Fig. 6. XRD spectra in 2θ ranges of (a) 27–32°, and (b) 72–75° (deconvoluted) for heat treated YSZ (204NS-1) for 100 h at 1300 °C. The differential (residual) plot for the deconvoluted profile is included ($R_{min} = 0.02\%$).

Table 4
Phase constitution of heat treated detached thermal barrier coatings.

Top coat/heat treatment	Phases (%)					
	Monoclinic *m*	Cubic *c*	Tetragonal *t*	Tetragonal t_1 (low-yttria)	Tetragonal t_2 (high-yttria)	Pyrochlore *p*
204NS-1/100 h at 1300 °C		46	–	35	19	–
Y_2O_3 (wt%)		13		1.7	6.3	
204NS/50 h at 1300 °C	2.9	29.5	–	23.2	44.4	–
Y_2O_3 (wt%)		10		1.6	6.7	
SPM6-2444/50 h at 1300 °C		11	89			–
SPM6-2444/100 h at 1350 °C	2	30	68			–
AE8321/50h at 1350 °C		39.2		37.3	12.5	11
AE8170/50 h at 1350 °C		32		55	13	–
Y_2O_3 (wt%)		14		1.8	6.6	
AE9018/50 h at 1300 °C		17	–	35	48	–
Y_2O_3 (wt%)		14.6		1.7	6.7	

composed of non-transformable t' should decompose at high temperature, to a mixture of high-yttria cubic and low-yttria tetragonal phases. On cooling to room temperature, the high-yttria high temperature cubic phase may be retained, or it may transform to a high-yttria tetragonal phase. On the other hand, the high temperature, low-yttria tetragonal phase, upon cooling might transform to a non-transformable tetragonal phase, t', or to a transformable tetragonal phase that may transform to monoclinic depending on the cooling rate, yttria content and grain size.[49,50] Previous investigations[49,50] have shown that the non-transformable t' phase decomposes after annealing heat treatments to a mixture of a high-yttria cubic phase and a low-yttria t'_1 tetragonal phase via an intermediate high-yttria t'_2 phase. The estimated percentages of the phases present in the current samples (and the yttria content in each phase) are shown in Table 4. The percentage of yttria in the tetragonal and cubic phases was deduced from the lattice parameters of each phase, according to empirical equations (see Eqs. (4) and (5)). The t'_1 low-yttria tetragonal phase has a composition of 1.7 wt% Y_2O_3, the high-yttria cubic (*c*) has 13 wt% Y_2O_3 and the t'_2 tetragonal phase has a composition of 6.3 wt% Y_2O_3. The t' gradually decomposes at high temperature into the equilibrium high-yttria cubic and low-yttria tetragonal phases equilibrium, but total decomposition is not achieved after 100 h and some intermediate t'_2 is still present. Decomposition occurs by gradual segregation of the yttria into lower and higher yttria regions, with corresponding changes in the *c*/*a* ratio. Of course, it must be recognized that some changes in phase constitution, and possibly in the composition of the phases, might have occurred during cooling to room temperature. The cubic phase formed at high temperature is retained at room temperature and contains about 13 wt% yttria, which agrees more or less with the phase diagram, which suggests that at 1300 °C the equilibrium concentration of the cubic phase should be about 12 wt%. This concentration exceeds the compositional limit of the t' phase and hence the cubic phase *c* is retained to room temperature.[12,49]

The 204NS YSZ top coat was heat treated for 50 h at 1300 °C. The evolution of the phase content can be seen in Fig. 7. After 1 h at 1300 °C, the coating is still predominantly t', but the peaks appear to broaden. This is probably caused by compositional differences in the tetragonal phase due to gradual diffusion of yttria, and corresponding changes in the lattice parameters. After 10 h of heat treatment, further broadening of the tetragonal peaks is apparent and a small additional peak appears which can be identified as the cubic peak. The trend continues for 20 h of heat treatment and after 50 h it is possible to recognize two distinct tetragonal phases and the cubic phase. Fig. 8b shows the deconvoluted profile the of 204NS YSZ top coat after heat treatment for 50 h at 1300 °C. The t' phase has also decomposed into a mixture of low-yttria tetragonal t'_1 high-yttria cubic *c* and t'_2 with an intermediate yttria composition. The percentages of each phase present are summarized in Table 4. As heat treatment progresses,

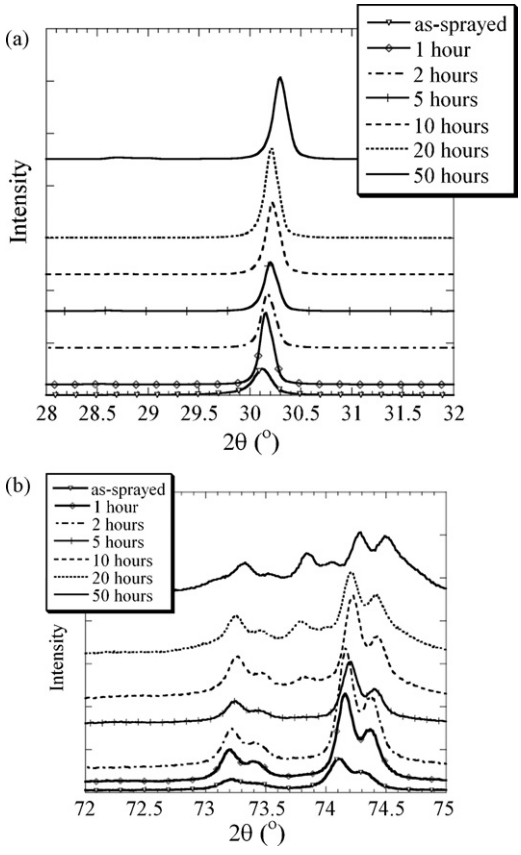

Fig. 7. XRD spectra in 2θ ranges of (a) 27–32°, and (b) 72–75° showing phase evolution for heat treated YSZ (204NS) up to 50 h at 1300 °C.

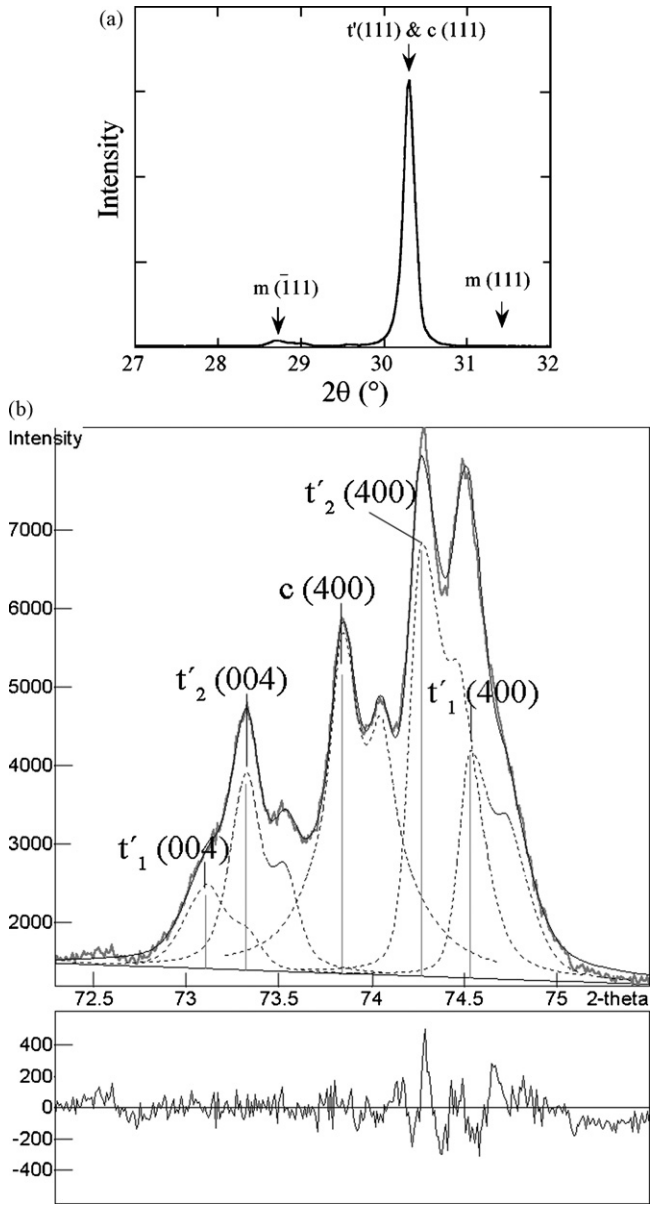

Fig. 8. XRD spectra in 2θ ranges of (a) 27–32°, and (b) 72–75° (deconvoluted) for heat treated YSZ (204NS) for 50 h at 1300 °C. The differential (residual) plot for the deconvoluted profile is included (R_{min} = 0.13%).

the amount of intermediate yttria t'_2 tetragonal phase appears to gradually decrease, while the low-yttria t'_1 and high-yttria cubic phases c appear to increase. Comparing the percentages of phases present in this top coat to those present in the YSZ 204NS-1 top coat after heat treatment for 100 h at 1300 °C, the amount of cubic and low-yttria phases present is less in this top coat than in the YSZ 204NS-1, since the longer heat treatment has allowed more decomposition of the high-yttria t'_2 tetragonal phase. A trace of monoclinic phase is also evident (Fig. 8a), which has probably resulted from the transformation of some of the low-yttria t'_1 tetragonal phase during cooling to room temperature.

It is not clear why there is some monoclinic phase present in the YSZ 204NS top coat, while none is present in the YSZ 204NS-1 top coat, which has the higher impurity content. The tetragonal-to-monoclinic transformation is associated with a volume increase which can be detrimental for the failure of TBCs, although the amount of monoclinic phase (2.9%) present in the YSZ 204NS top coat in the current study is probably not significant enough to cause failure. It is worth noting, however, that the presence of SiO_2 impurities probably aids the phase stability in the YSZ 204NS-1 powder.

The Al_2O_3-doped-YSZ top coat (AE9018) was heat treated for 50 h at 1300 °C. This top coat has a similar composition and impurity level to the YSZ 204NS top coat, with Al_2O_3 being the only significant difference. The t' tetragonal phase decomposed to a mixture of low-yttria tetragonal t'_1 high-yttria cubic c and t'_2 with an intermediate yttria composition (Fig. 9). Even though the amount of cubic phase present was slightly less than the corresponding level in the YSZ 204NS top coat given the same

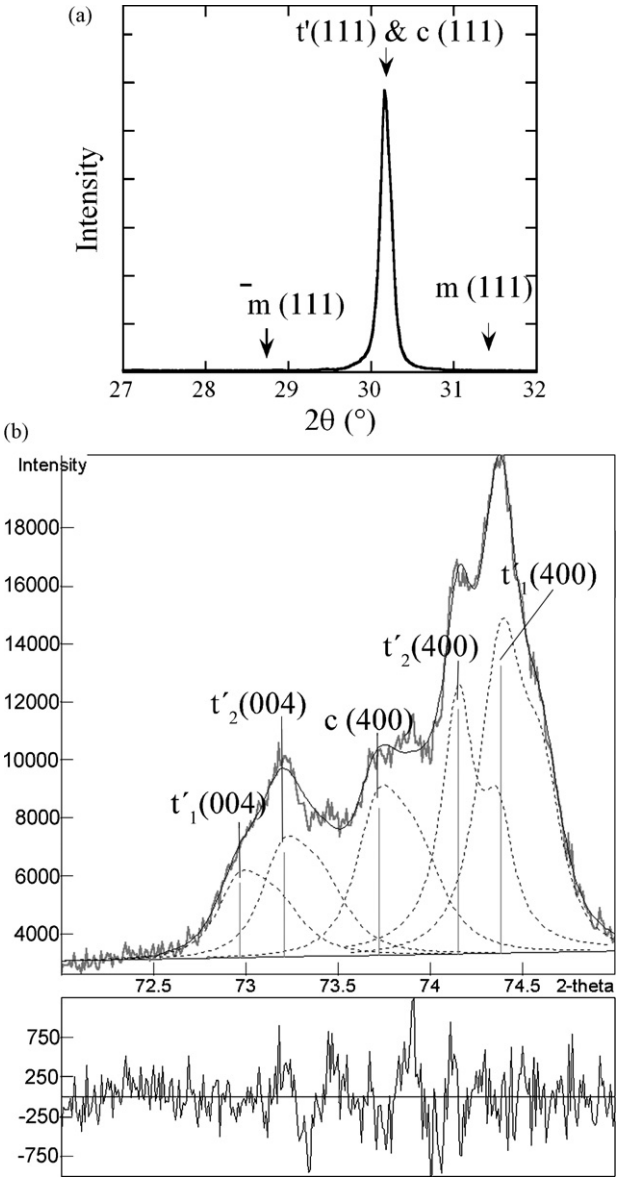

Fig. 9. XRD spectra in 2θ ranges of (a) 27–32°, and (b) 72–75° (deconvoluted) for heat treated Al_2O_3-doped-YSZ (AE9018) for 50 h at 1300 °C. The differential (residual) plot for the deconvoluted profile is included (R_{min} = 0.26%).

heat treatment, it can not be said conclusively that the tetragonal phase appears to be more stable. In both top coats, the percentage of intermediate yttria t'_2 tetragonal phase is comparable, indicating that approximately the same amount of decomposition into high and low-yttria containing regions took place. However, it should be pointed out that the gradual decomposition of the t'_2 into higher and lower yttria regions often results in compositional variations, which make the observed peaks broader, but not necessarily identifiable as distinct phases of low and high-yttria content. Therefore deconvolution of the X-ray pattern presented in Fig. 9b presented great difficulty and it is possible that alternative interpretations of the peaks observed might also be applicable. Nevertheless, it can be concluded that the addition of alumina does not appear to make a significant difference to the stabilization of the tetragonal phases, although it appears that yttria diffusion appears to be slightly slower in Al_2O_3-doped-YSZ than in YSZ top coats with similar amounts of other impurities.

The Al_2O_3-doped-YSZ top coat (AE8170), which has a very similar composition to the Al_2O_3-doped-YSZ AE9018 top coat, was heat treated for 50 h at 1350 °C (Fig. 10). The percentage of cubic phase present in this case is slightly higher than that observed in the AE9018 top coat that was heat treated at a slightly lower temperature (Table 4). This highlights the influence of the heat treatment temperature on the decomposition rate of the t' phase into its equilibrium phase. The temperature difference of 50 °C significantly affects the percentage of cubic phase formed. As mentioned previously, compositional variations resulting from the progressive diffusion of yttria into high- and low-yttria regions results in broadening of the observed peaks and sometimes it is difficult to differentiate distinct phases and distinguish this from a single tetragonal phase exhibiting a broad peak. In the current case, is possible to deconvolute the observed pattern (Fig. 10b) into either a low-yttria t'_1, high-yttria cubic c and intermediate t'_2 yttria phases or simply into a tetragonal and a cubic phase. Another possibility is the existence of a mixture of phases with small compositional variations. Thus X-ray analysis cannot in this case be reliably used to establish the phase constitution. Other techniques, such as TEM might be useful to provide further information.

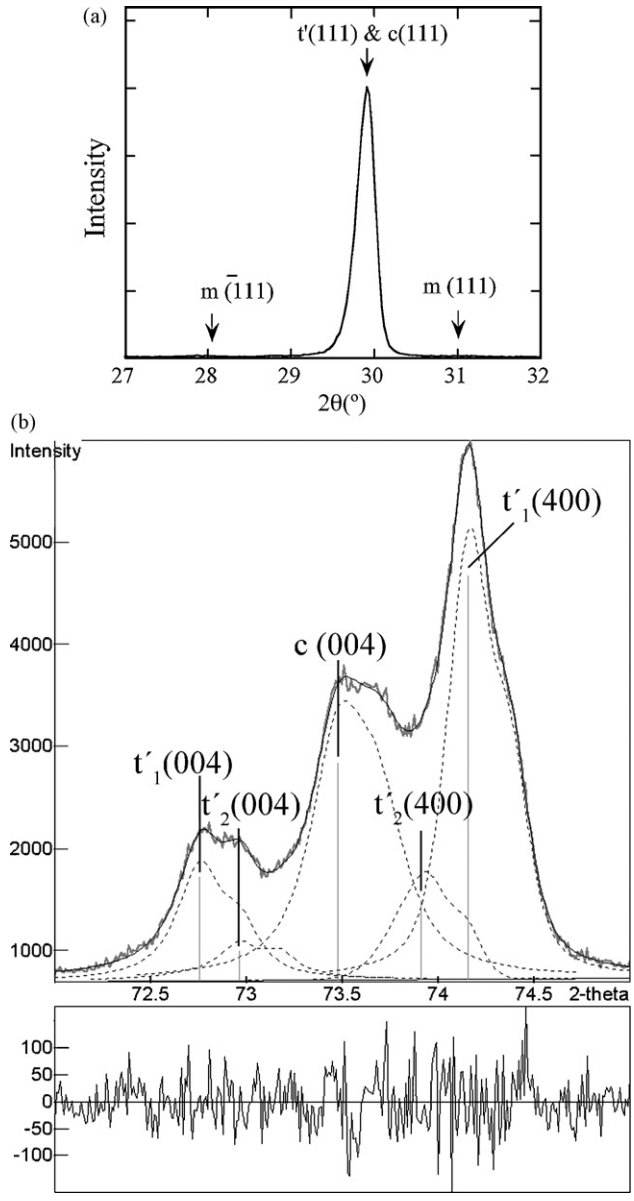

Fig. 10. XRD spectra in 2θ ranges of (a) 27–32°, and (b) 72–75° (deconvoluted) for heat treated Al_2O_3-doped-YSZ (AE8170) for 50 h at 1350 °C. The differential (residual) plot for the deconvoluted profile is included (R_{min} = 0.05%).

3.2.2. *Dysprosia-stabilized zirconia top coats*

The DSZ top coat (SPM6-2444) decomposes slowly during heat treatment and gradually a cubic phase appears. The X-ray spectrum after 50 h at 1300 °C is difficult to deconvolute and hence it can not be said with certainty whether there are one or more tetragonal phases present (Fig. 11a). It is almost certain that small compositional variations in the cubic and tetragonal intermediate phases result in the observed broadening of the base of the two tetragonal peaks. According to the phase diagram of this system,[51] both the pyrochlore (p) phase $Dy_2Zr_2O_7$ and the zirconia solid solution phases co-exist when the concentration of Dy_2O_3 is above 15 mol.%. No pyrochlore phase was formed in the present work, due to the relatively low mol.% of Dy_2O_3 present. The X-ray spectrum of DSZ after heat treatment at 1350 °C for 100 h shows a considerably higher amount of the cubic phase c (Fig. 11b). Since the temperature and heat treatment time were higher, it comes as no surprise that there is more cubic phase present. A trace of monoclinic is also present (Fig. 12). There are no well-established equations relating the peak position to the phase composition for dysprosia (as there are for yttria) and hence is not possible to calculate the dysprosia content in these phases. From the present results it can be concluded that for the current amount of stabilizer (3.58 mol.%), dysprosia successfully stabilized the tetragonal phase in plasma sprayed coatings. After heat treatment a certain amount of decomposition occurred, similar to that in conventional YSZ top coats.

3.2.3. *Yttria–lanthana-stabilized zirconia top coats*

In the YLaSZ top coat after heat treatment, the tetragonal phases initially present in the as sprayed coating decompose into

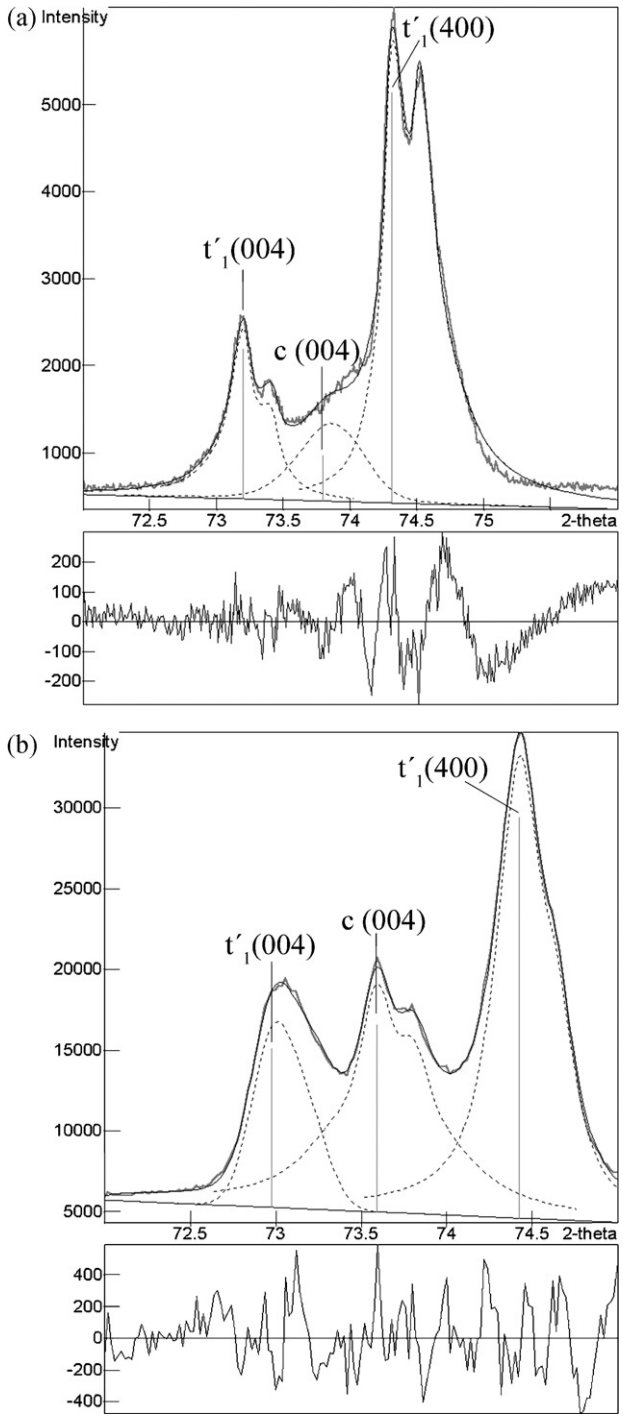

Fig. 11. XRD spectra (deconvoluted) in 2θ ranges of 72–75° for heat treated DSZ (SMP6–2444) at (a) 1300 °C for 50 h and (R_{min} = 0.28%) (b) at 1350 °C for 100 h (R_{min} = 0.03%). The differential (residual) plots for the deconvoluted profiles are included.

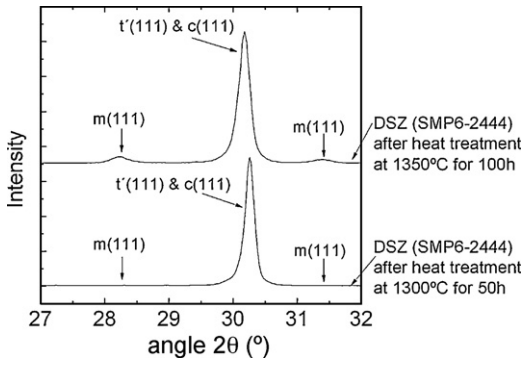

Fig. 12. XRD spectra in 2θ ranges of 27–32° for heat treated DSZ (SMP6–2444) at 1300 °C for 50 h and at 1350 °C for 100 h.

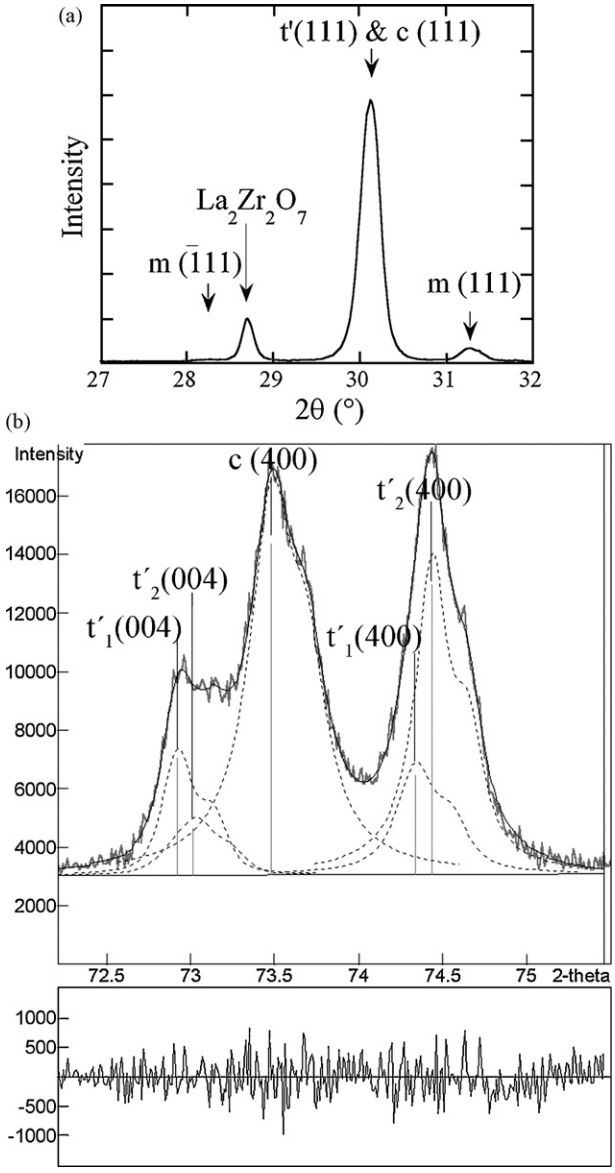

Fig. 13. XRD spectra in 2θ ranges of (a) 27–32°, and (b) 72–75° (deconvoluted) for heat treated YLaSZ (AE8321) for 50 h at 1350 °C. The differential (residual) plot for the deconvoluted profile is included (R_{min} = 0.19%).

a mixture of tetragonal, cubic and the cubic pyrochlore (p) phase $La_2Zr_2O_7$ as shown in Fig. 13 (for deconvolution considering one cubic and one tetragonal phase R_{min} = 0.79% whereas considering two tetragonal and one cubic phase is R_{min} = 0.19%). The percentages of each phase were calculated using Rietveld analysis (see Table 4). The presence of the pyrochlore phase $La_2Zr_2O_7$ in LaSZ has been reported previously.[25] When both

lanthana and yttria are present, it appears that decomposition of the lanthana-doped zirconia and yttria-doped zirconia occurs simultaneously and a mixture of tetragonal, cubic and pyrochlore phases is present. The formation of the pyrochlore phase *p* accompanies a volume increase, which is thought to enhance the tetragonal-to-monoclinic phase transformation.[24,52] The presence of both lanthana and yttria makes it difficult to estimate the stabilizer content from the peak position. $La_2Zr_2O_7$ top coats consisting of the pyrochlore-structure have been proposed as a promising new TBC materials,[27,28,53–55] because of their stable structure up to the melting points and lower thermal conductivity. Although, these top coats have lower cycling life that YSZ top coats due to their lower CTE. However, in the present study the YLaSZ top coat was not phase stable, probably due to the presence of both yttria and lanthana and it decomposed after heat treatment forming a mixture of pyrochlore, cubic and tetragonal phases.

4. Conclusions

Exposure to high temperature induced phase changes in all top coats studied, including top coats doped with yttria, and those doped with ceria, yttria–lanthana and dysprosia. These phase changes may affect the microstructure and perhaps the stress state in TBCs. Even though the conventional YSZ as-sprayed top coats consited entirely of the so-called "non-transformable tetragonal" t' phase, at temperatures above 1300 °C they decompose to their equilibrium tetragonal (*t*) and cubic (*c*) phases. On cooling to room temperature the coatings consisted of mixtures of cubic (*c*) phases, and tetragonal phases (t'_1 and t'_2). The presence of SiO_2 and Al_2O_3 impurities appeared to decrease the rate of decomposition of the non-transformable tetragonal phase. Similar conclusions can be drawn for zirconia plasma sprayed coatings with dysprosia stabilizer. Specifically, dysprosia, in the amount present in the current study (3.58 mol.%), successfully stabilized the tetragonal phase in plasma sprayed zirconia coatings. However, after heat treatment, a certain amount of decomposition occurred, similar to that in conventional YSZ top coats. In the case where two different stabilizing oxides were used, yttria and lanthana, the as-sprayed YLaSZ top coats consisted of two tetragonal phases, rather than a single non-trasformable tetragonal phase. After heat treatment, the YLaSZ top coat was not phase stable, probably due to the presence of both yttria and lanthana and it decomposed to a mixture of cubic (*c*), high-yttria tetragonal phases (t'_1 and t'_2), and the pyrochlore (*p*) phase. Finally, when the tetravalent Ce^{4+} ion was employed in order to stabilize zirconia, a different behaviour was observed. The Ce^{4+} ion in the CSZ top coat was reduced to Ce^{3+} during annealing at 500 °C in vacuum. As a result, the non-transformable tetragonal t' phase decomposed into the cubic (*c*) phase. It can be concluded that the cerium valence state has a great influence on the phase composition, and it is believed to affect the stress state in the coating. For zirconia-based plasma sprayed top coats, the stabilization mechanism seems to be dependent on the amount and nature of the stabilizing oxide used.

Acknowledgements

The author acknowledges the financial support received from Sulzer Metco, the Cambridge European Trust and from EPSRC for the realization of this work. There have been many useful discussions with industrial partners, particularly Jason Doesburg, Andrew Nicoll, Mitch Dorfman and Keith Harrison (Sulzer Metco).

References

1. Herman, H. and Shankar, N. R., Survivability of thermal barrier coatings. *Mater. Sci. Eng.*, 1987, **88**, 69–74.
2. Langjahr, P. A., Oberacker, R. and Hoffmann, M. J., Long-term behavior and application limits of plasma-sprayed zirconia thermal barrier coatings. *J. Am. Ceram. Soc.*, 2001, **84**, 1301–1308.
3. Fabris, S., Paxton, A. T. and Finnis, M. W., A stabilization mechanism of zirconia based on oxygen vacancies only. *Acta Mater.*, 2002, **50**, 5171–5178.
4. Ho, S. M., On the structural chemistry of zirconium-oxide. *Mater. Sci. Eng.*, 1982, **54**, 23–29.
5. Li, P., Chen, I. W. and Pennerhahn, J. E., Effect of dopants on zirconia stabilization – an X-ray-absorption study. 1. Trivalent dopants. *J. Am. Ceram. Soc.*, 1994, **77**, 118–128.
6. Porter, D. L. and Heuer, A. H., Microstructural development in Mgo-partially stabilized zirconia (Mg-PSZ). *J. Am. Ceram. Soc.*, 1979, **62**, 298–305.
7. Bennett, A., Properties of thermal barrier coatings. *Mater. Sci. Technol.*, 1986, **2**, 257–261.
8. Maier, R. D., Scheuermann, C. M. and Andrews, C. W., Degradation of a 2-layer thermal barrier coating under thermal cycling. *Am. Ceram. Soc. Bull.*, 1981, **60**, 555–560.
9. Brandon, J. R. and Taylor, R., Phase-stability of zirconia-based thermal barrier coatings. 2. Zirconia ceria alloys. *Surf. Coat. Technol.*, 1991, **46**, 91–101.
10. Choi, H., Kim, H. and Lee, C., Phase evolutions of plasma sprayed ceria and yttria stabilized zirconia thermal barrier coating. *J. Mater. Sci. Lett.*, 2002, **21**, 1359–1361.
11. Lee, E. Y., Sohn, Y. H., Jha, S. K., Holmes, J. W. and Sisson, R. D., Phase transformations of plasma-sprayed zirconia–ceria thermal barrier coatings. *J. Am. Ceram. Soc.*, 2002, **85**, 2065–2071.
12. Moon, J., Choi, H., Kim, H. and Lee, C., The effects of heat treatment on the phase transformation behavior of plasma-sprayed stabilized ZrO_2 coatings. *Surf. Coat. Technol.*, 2002, **155**, 1–10.
13. Wilden, J. and Wank, A., Application study on ceria based thermal barrier coatings. *Materialwissenschaft Und Werkstofftechnik*, 2001, **32**, 654–659.
14. Dalmaschio, R., Scardi, P., Lutterotti, L. and Ingo, G. M., Influence of Ce^{3+}/Ce^{4+} ratio on phase-stability and residual-stress field in ceria yttria stabilized zirconia plasma-sprayed coatings. *J. Mater. Sci.*, 1992, **27**, 5591–5596.
15. Portinha, A., Teixeira, V., Carneiro, J., Costa, M. F., Barradas, N. P. and Sequeira, A. D., Stabilization of ZrO_2 PVD coatings with Gd_2O_3. *Surf. Coat. Technol.*, 2004, **188**, 107–115.
16. Rebollo, N. R., Fabrichnay, O. and Levi, C. G., Phase stability of Y + Gd co-doped zirconia. *Zeitschrift Fur Metall.*, 2003, **94**, 163–170.
17. Khor, K. A. and Yang, J., Lattice parameters, tetragonality (*c*/*a*) and transformability of tetragonal zirconia phase in plasma-sprayed ZrO_2–Er_2O_3 coatings. *Mater. Lett.*, 1997, **31**, 23–27.
18. Khor, K. A. and Yang, J., Plasma sprayed ZrO_2–Sm_2O_3 coatings: lattice parameters, tetragonality (*c*/*a*) and transformability of tetragonal zirconia phase. *J. Mater. Sci. Lett.*, 1997, **16**, 1002–1004.
19. Khor, K. A. and Yang, J., Transformability of t-ZrO_2 and lattice parameters in plasma sprayed rare-earth oxides stabilized zirconia coatings. *Scr. Mater.*, 1997, **37**, 1279–1286.
20. Jones, R. L., Reidy, R. F. and Mess, D., Scandia, yttria-stabilized zirconia for thermal barrier coatings. *Surf. Coat. Technol.*, 1996, **82**, 70–76.
21. Leoni, M., Jones, R. L. and Scardi, P., Phase stability of scandia–yttria-stabilized zirconia TBCs. *Surf. Coat. Technol.*, 1998, **109**, 107–113.

22. Hamacha, R., Fauchais, P. and Nardou, F., Influence of dopant on the thermal properties of two plasma-sprayed zirconia coatings. 1. Relationship between powder characteristics and coating properties. *J. Ther. Spray Technol.*, 1996, **5**, 431–438.
23. Yoshimura, M., Phase-stability of zirconia. *Am. Ceram. Soc. Bull.*, 1988, **67**, 1950–1955.
24. Andrievskaya, E. R. and Lopato, L. M., Influence of composition on the T–M transformation in the systems ZrO_2–Ln_2O_3 (Ln = La, Nd, Sm, Eu). *J. Mater. Sci.*, 1995, **30**, 2591–2596.
25. Bastide, B., Odier, P. and Coutures, J. P., Phase-equilibrium and martensitic-transformation in lanthana-doped zirconia. *J. Am. Ceram. Soc.*, 1988, **71**, 449–453.
26. Thangadurai, P., Sabarinathan, V., Bose, A. C. and Ramasamy, S., Conductivity behaviour of a cubic/tetragonal phase stabilized nanocrystalline La_2O_3–ZrO_2. *J. Phys. Chem. Solids*, 2004, **65**, 1905–1912.
27. Vassen, R., Cao, X. Q., Tietz, F., Basu, D. and Stover, D., Zirconates as new materials for thermal barrier coatings. *J. Am. Ceram. Soc.*, 2000, **83**, 2023–2028.
28. Cao, X. Q., Vassen, R. and Stoever, D., Ceramic materials for thermal barrier coatings. *J. Eur. Ceram. Soc.*, 2004, **24**, 1–10.
29. Tsipas, S. A., Golosnoy, I. O., Damani, R. and Clyne, T. W., The effect of a high thermal gradient on sintering and stiffening in the top coat of a thermal barrier coating system. *J. Ther. Spray Technol.*, 2004, **13**, 370–376.
30. Miller, R. A., Smialek, J. L. and Garlick, R. G., Phase stability in plasma-sprayed, partially stabilized zirconia–yttria. In *First International Conference on the Science and Technology of Zirconia, Science and Technology of Zirconia I*, ed. A. H. Heuer and L. W. Hobbs. American Ceramic Society, Cleveland, OH, 1980, pp. 241–253.
31. Toraya, H., Yoshimura, M. and Somiya, S., Calibration curve for quantitative-analysis of the monoclinic-tetragonal ZrO_2 system by X-ray-diffraction. *J. Am. Ceram. Soc.*, 1984, **67**, C119–C121.
32. Toraya, H., Yoshimura, M. and Somiya, S., Quantitative-analysis of monoclinic-stabilized cubic ZrO_2 systems by X-ray-diffraction. *J. Am. Ceram. Soc.*, 1984, **67**, C183–C184.
33. Wiles, D. B. and Young, R. A., A new computer-program for Rietveld analysis of X-ray-powder diffraction patterns. *J. App. Cryst.*, 1981, **14**, 149–151.
34. Scott, H. G., Phase relationships in zirconia–yttria system. *J. Mater. Sci.*, 1975, **10**, 1527–1535.
35. Heuer, A. H., Chaim, R. and Lanteri, V., The displacive cubic–tetragonal transformation in zro$_2$ alloys. *Acta Metall.*, 1987, **35**, 661–666.
36. Lanteri, V., Heuer, A. H. and Mitchell, T. E., Formation of tetragonal ZrO_2 in Y-PSZ. *Am. Ceram. Soc. Bull.*, 1984, **63**, 991.
37. Lanteri, V., Valentine, P., Heuer, A. H. and Mitchell, T. E., Precipitation of tetragonal ZrO_2 in Y-PSZ. *Am. Ceram. Soc. Bull.*, 1982, **61**, 808.
38. Miller, R. A., Garlick, R. G. and Smialek, J. L., Phase distributions in plasma-sprayed zirconia–yttria. *Am. Ceram. Soc. Bull.*, 1983, **62**, 1355–1358.
39. Sheu, T. S., Tien, T. Y. and Chen, I. W., Cubic-to-tetragonal (T') transformation in zirconia-containing systems. *J. Am. Ceram. Soc.*, 1992, **75**, 1108–1116.
40. Lakiza, S. M. and Lopato, L. M., Stable and metastable phase relations in the system alumina–zirconia–yttria. *J. Am. Ceram. Soc.*, 1997, **80**, 893–902.
41. Stough, M. A. and Hellmann, J. R., Solid solubility and precipitation in a single-crystal alumina–zirconia system. *J. Am. Ceram. Soc.*, 2002, **85**, 2895–2902.
42. Din, S. U. and Kaleem, A., Vickers hardness study of zirconia partially stabilized with lanthanide group oxides. *Mater. Chem. Phys.*, 1998, **53**, 48–54.
43. Yoshimura, M., Yashima, M., Noma, T. and Somiya, S., Formation of diffusionlessly transformed tetragonal phases by rapid quenching of melts in ZrO_2 rare earths $O_{1.5}$ systems. *J. Mater. Sci.*, 1990, **25**, 2011–2016.
44. Li, M. J., Feng, Z. C., Ying, P. L., Xin, Q. and Li, C., Phase transformation in the surface region of zirconia and doped zirconia detected by UV Raman spectroscopy. *Phys. Chem. Chem. Phys.*, 2003, **5**, 5326–5332.
45. Boutz, M. M. R., Winnubst, A. J. A. and Burggraaf, A. J., Yttria-ceria stabilized tetragonal zirconia polycrystals – sintering, grain-growth and grain-boundary segregation. *J. Eur. Ceram. Soc.*, 1994, **13**, 89–102.
46. Li, P. and Chen, I. W., Effect of dopants on zirconia stabilization – an X-ray-absorption study. 2. Tetravalent dopants. *J. Am. Ceram. Soc.*, 1994, **77**, 1281–1288.
47. Mastelaro, V. R., Briois, V., de Souza, D. P. F. and Silva, C. L., Structural studies of a ZrO_2–CeO_2 doped system. *J. Eur. Ceram. Soc.*, 2003, **23**, PII:S0955-2219(0902)00188-00187.
48. Langjahr, P. A., Oberacker, R. and Hoffmann, M. J., Long-term behaviour and application limits of plasma-sprayed CeO_2- and Y_2O_3-stabilized ZrO_2 thermal barrier coatings. *Materialwissenschaft Und Werkstofftechnik*, 2001, **32**, 665–668.
49. Brandon, J. R. and Taylor, R., Phase-stability of zirconia-based thermal barrier coatings. 1. Zirconia–yttria alloys. *Surf. Coat. Technol.*, 1991, **46**, 75–90.
50. Vanvalzah, J. R. and Eaton, H. E., Cooling rate effects on the tetragonal to monoclinic phase-transformation in aged plasma-sprayed yttria partially-stabilized zirconia. *Surf. Coat. Technol.*, 1991, **46**, 289–300.
51. Michel, D., Perezyjo, M. and Collongu, R., Study of order-disorder transformation of fluorite structure with pyrochlore type phases of formula $(1-X)$ ZrO_2–XLn_2O_3. *Mater. Res. Bull.*, 1974, **9**, 1457–1468.
52. Jang, J. W., Kim, D. J. and Lee, D. Y., Size effect of trivalent oxides on low temperature phase stability of 2Y-TZP. *J. Mater. Sci.*, 2001, **36**, 5391–5395.
53. Cao, X. Q., Vassen, R., Jungen, W., Schwartz, S., Tietz, F. and Stover, D., Thermal stability of lanthanum zirconate plasma-sprayed coating. *J. Am. Ceram. Soc.*, 2001, **84**, 2086–2090.
54. Cao, X. Q., Vassen, R., Tietz, F. and Stoever, D., New double-ceramic-layer thermal barrier coatings based on zirconia–rare earth composite oxides. *J. Eur. Ceram. Soc.*, 2006, **26**, 247–251.
55. Vassen, R., Dietrich, M., Lehmann, H., Cao, X., Pracht, G., Tietz, F. *et al.*, Development of oxide ceramics for an application as TBC. *Materialwissenschaft Und Werkstofftechnik*, 2001, **32**, 673–677.
56. Shannon, R. D., Revised effective ionic-radii and systematic studies of interatomic distances in halides and chalcogenides. *Acta Crystallogr. A*, 1976, **32**, 751–767.